

Long Term Optical Photometry of the Black Hole Binary J1118+480

Lorena Monroy¹, Paul A. Mason^{1,2}, Edward L. Robinson³

and

Rob I. Hynes⁴

ABSTRACT

The black hole LMXB J1118+480 was observed using the Argos photometer on the 2.1 m telescope of McDonald Observatory on 30 nights from 2004 to 2012. Integration times were 10s and a broad-band (BVR) filter was used. All the light curves display a two-humped orbital modulation that has been interpreted as ellipsoidal variations. In addition, flickering is observed predominately during the bright phases of the orbital variation. The bright phase intensity and flickering variability is found to change from run to run over the course of our observations, while both minima in the ellipsoidal variations remain relatively constant. High quality light curves covering many full orbital cycles and a baseline of eight years allow for an improved orbital ephemeris.

Subject headings: binary systems: X-ray binaries, KV UMa, XTE J1118+480

1. Introduction

Binary star systems are made up of two objects that revolve around one center of mass that is highly concentrated. Low mass X-ray binaries (LMXB) is where one component is either a black hole or neutron star with a donor star. The black hole binary XTE J1118+480 was first discovered with the Rossi X-Ray Timing Explorer (RXTE) All-Sky Monitor (ASM) when an X-ray emission outburst was detected on March 29, 2000 by Remillard et al. (2000). The optical counterpart was found on March 30, 2000 by Uemura et al. (2000a). An orbital period of about $P = 0.170$ days was found in 2000 (Patterson et al. (2000), Uemura et al. (2000b), and Cook et al. (2000)).

In 2001, a spectroscopy orbital period $P = 0.169930 \pm 0.000004$ days was found by Wagner et al. (2001) with the 6.5 m Multiple Mirror Telescope and 4.2 m William Herschel Telescope. The orbital period found was when Wagner et al. (2001) first tested by the phasing of the radial velocity on photometric period of 0.17 days by Uemura et al. (2000b). The same year, McClintock et al. (2001), gave also a period of $P = 0.17013 \pm 0.00010$ days. Later in 2004, Torres et al. (2004) gave an orbital period of 0.1699339 ± 0.0000002 days using spectroscopic observations. In this paper, we present optical results for 30 nights from 2004 April to 2012 May.

¹Department of Physics, University of Texas at El Paso, El Paso, TX 79968, USA

²Department of Mathematics and Physical Sciences, New Mexico State University - DACC, Las Cruces, NM 88003, USA

³Department of Astronomy, University of Texas at Austin, 1 University Station, Austin, TX 78712, USA

⁴Department of Physics and Astronomy, Louisiana State University, Baton Rouge, LA 70803, USA

2. Observations & Analysis

30 nights of data was taken from the McDonald Observatory 82-inch telescope. The dates of data taken were from 2004 April 17-25, 2005 May 5 & 9, 2010 May 8-16, 2010 June 10-18, 2011 June 2, 2012 February 21-27, and 2012 May 16-22 (seen in **Table 1**, UT). The data taken for the years 2004 and 2005 was made available by Rob Hynes.

$$T = T_0 + PE$$

$$T_0 = \text{HJD } 2453112.7673 \pm 0.008$$

$$P = 0.16993398 \pm 0.00000009 \text{ days}$$

3. Conclusion

The orbital period found from the photometric data is $P = 0.16993398 \pm 9$ days. The flickering is evidence for continued mass transfer in the system. The lack of detectable X-ray flux from J1118+480 means that most of transferred mass is retained in the outer accretion disk and not flowing down to the inner accretion disk. The strong and immediate correlation between the flickering amplitude and the mean flux at optical wavelengths shows that most or all the accretion-induced optical flux (as opposed to the flux from the secondary star) is being generated locally in the outer disk. Again, this is evidence that most of the transferred mass is being retained in the outer disk. this behavior is expected in the disk instability model for X-ray transients. Finally, the mass transfer is clearly distorting the ellipsoidal variations since the asymmetric and rapidly-variable orbital light curve cannot be produced by pure ellipsoidal variations. Furthermore, the amount of mass transfer and the amount of distortion varies strongly on time scales as short as one day.

We thank Rob Hynes, who generously made available his XTE J118+480 raw data for 2004 and 2005. This research is supported by a National Science Foundation (NSF), Partnership in Astronomy and Astrophysics Research and Education (PAARE) Grant No. 0958783 to the University of Texas at El Paso (UTEP).

REFERENCES

- Brocksopp, C., Jonker, P. G., Maitra, D., Krimm, H. A., Pooley, G. G., Ramsay, G., & Zurita, C., 2010, R. Astron. Soc., 404, 908
- Cook, L., Patterson, J., Buczynski, D., & Fried, R., 2000, IAU Circ. No 7397, 2
- Dubus, G., Kim, R. S. J., Menou, K., Szkody, P., & Bowen, D. V., 2001, ApJ, 553, 307
- Fragos, T., Williams, B., Ivanova, N., & Kalogera, V., 2007, AIP, 673, 678
- Garcia, M., Brown, W., Pahre, M., McClintock, J., Callanan, P., & Garnavich, P., 2000, IAU Circ. No 7392, 2
- Gelino, D. M., Balman, S., Kizilođlu, U., Yilmaz, A., Kalemci, E., & Tomsick, J. A., 2006, ApJ, 642, 438

- Hynes, R. I., Mauche, C. W., Haswell, C. A., Shrader, C. R., Cui, W., & Chaty, S., 2000, *ApJ*, 539, L37
- Hynes, R. I., Robinson, E. L., Pearson, K. J., Gelino, D. M., Cul, W., Xue, Y. Q., Wood, M. A., Watson, T. K., Winget, D. E., & Silver, I. M., 2006, *ApJ*, 651, 401
- Khargharia, J., Froning, C. S., Robinson, E. L. & Gelino, D. M. 2013, *Astron. Journal*, 145, 21
- Khruzina, T. S., Cherepashchuk, A. M., Bisikalo, D. V., Boyarchuck, A. A., & Kuznetsov, O. A., 2005, *Astron. Rep.*, 49, 79
- Malzac, J., Belloni, T., Spruit, H. C., & Kanbach, G., 2003, *A&A*, 407, 335
- McClintock, J. E., Garcia, M. R., Caldwell, N., Falco, E. E., Garnavich, P. M., & Zhao, P., 2001, *ApJ*, 551, L147
- Patterson, J., Fried, R., Harvey, D., Cook, L., Masi, G., Kemp, J., Hannon, J., Buczynski, D., Vanmunster, T., Pidgley, L., Maxted, P., & Araujo-Betancor, S., 2000, *IAU Circ. No 7412*, 2
- Reis, R. C., Miller, J. M., & Fabian, A. C., 2009, *Astron. Soc.*, 395, L52
- Remillard, R., Morgan, E., Smith, D., & Smith, E., 2000, *IAU Circ. No 7389*, 2
- Shahbaz, T., Dhillon, V. S., Marsh, T. R., Casares, J., Zurita, C., Charles, P. A., Haswell, C. A., & Hynes, R.I., 2005, *Astron. Soc.*, 362, 975
- Torres, M. A. P., Callanan, P. J., Garcia, M. R., Zhao, P., Laycock, S., & Kong, A. K. H., 2004, *ApJ*, 612, 1026
- Uemura, M., Kato, T., & Yamaoka, H., 2000a, *IAU Circ. No 7390*, 1
- Uemura, M., Kato, T., Matsumoto, K., Yamaoka, H., Takamizawa, K., Sano, Y., Haseda, K., Cook, L. M., Buczynski, D., & Masi, G., 2000b, *PASJ*, in press (astro-ph/0004245)
- Wagner, R. M., Foltz, C. B., Shahbaz, T., Casares, J., Charles, P. A., Starrfield, S. G., & Hewett, P., 2001, *ApJ*, 556, 42
- Wren, J., Akerlof, C., Balsano, R., Bloch, J., Borozdin, K., Casperson, D., Gisler, G., Kehoe, R., Lee, B. C., Marshall, S., McKay, T., Preidhorsky, W., Rykoff, E., Smith, D., Trudolyubov, S., & Vestrand, W. T., 2001, *ApJ*, 557, L97

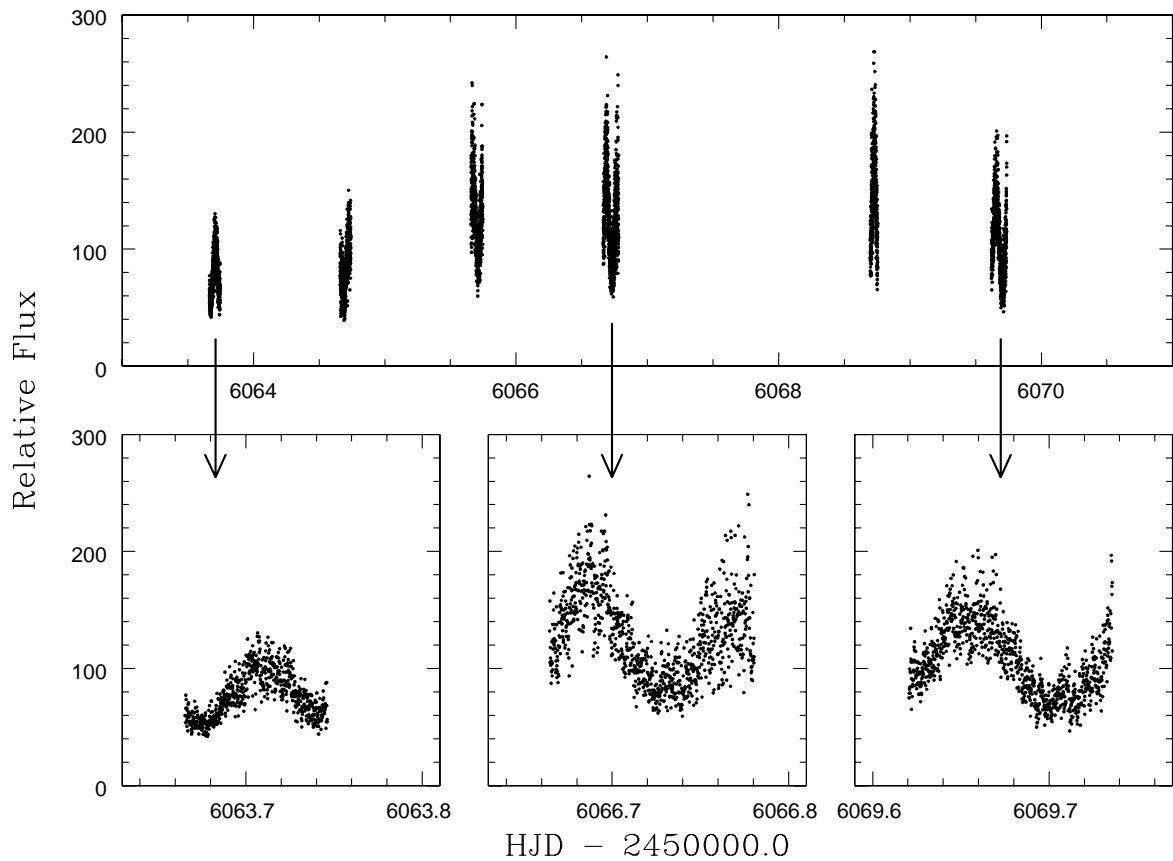


Fig. 1.— Light curves from 6 nights in May 2012 are shown. The increase of brightness from the 2nd to 3rd nights, in the upper plot, coincided with an increase in amplitude and flickering as seen in the lower close-ups.

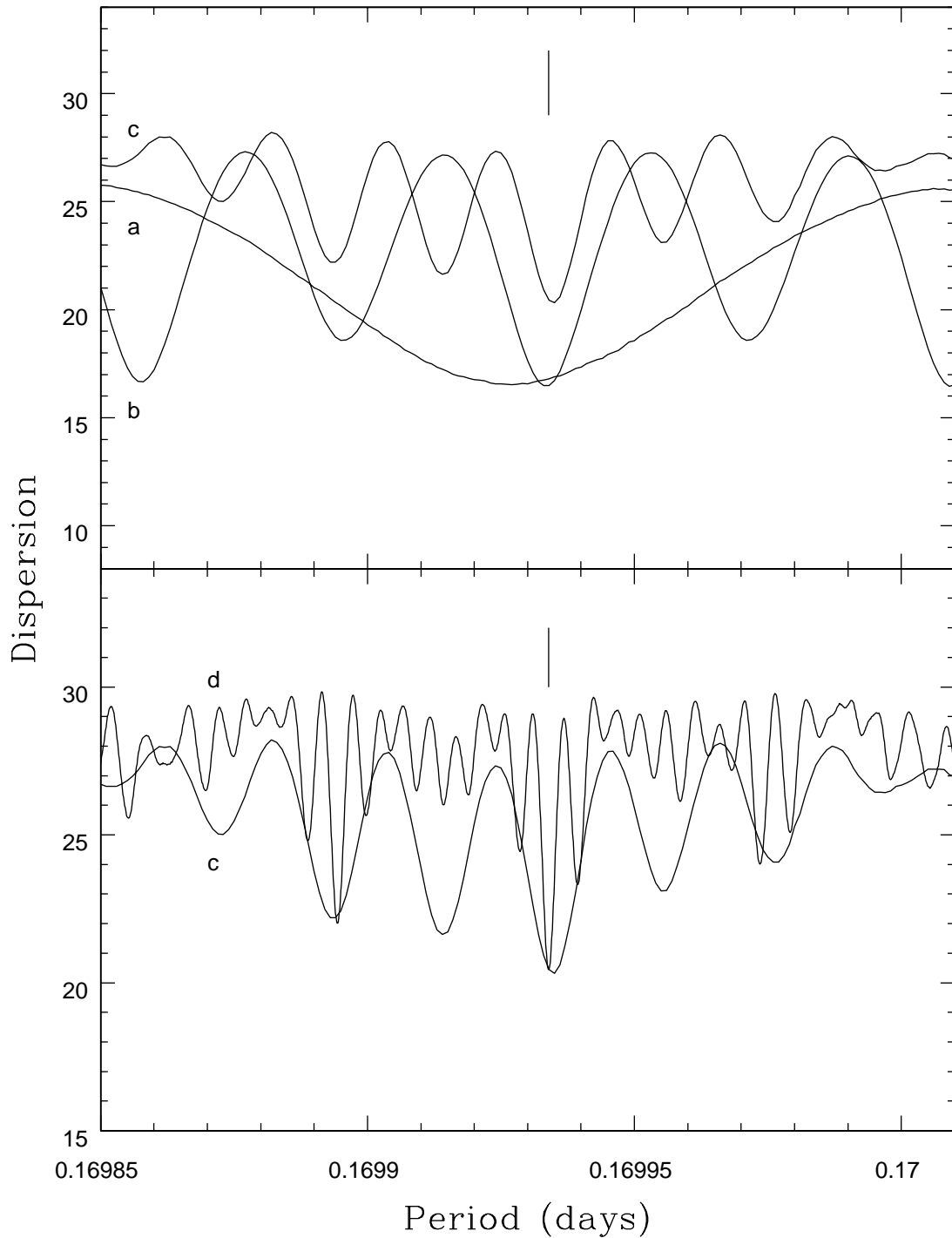


Fig. 2.— PDM Periodogram. Intensity of the light curves were normalized to make a smoother light curve so data could be run into the PDM to show the change of orbital period on one year data (2012), two year data (2004 and 2005), three year data (2010, 2011, and 2012), and five year data (2004, 2005, 2010, 2011, and 2012). The arrow represents the position of the orbital period $P = 0.1699339 \pm 0.0000002$ by Torres et al. (2004). The width of the arrowhead represents the error of Torres et al. (2004) orbital period. The top graph shows the one, two, and three year data. The bottom graph shows the three and five year data. The graph gives an estimate PDM of $P = 0.1699338$.

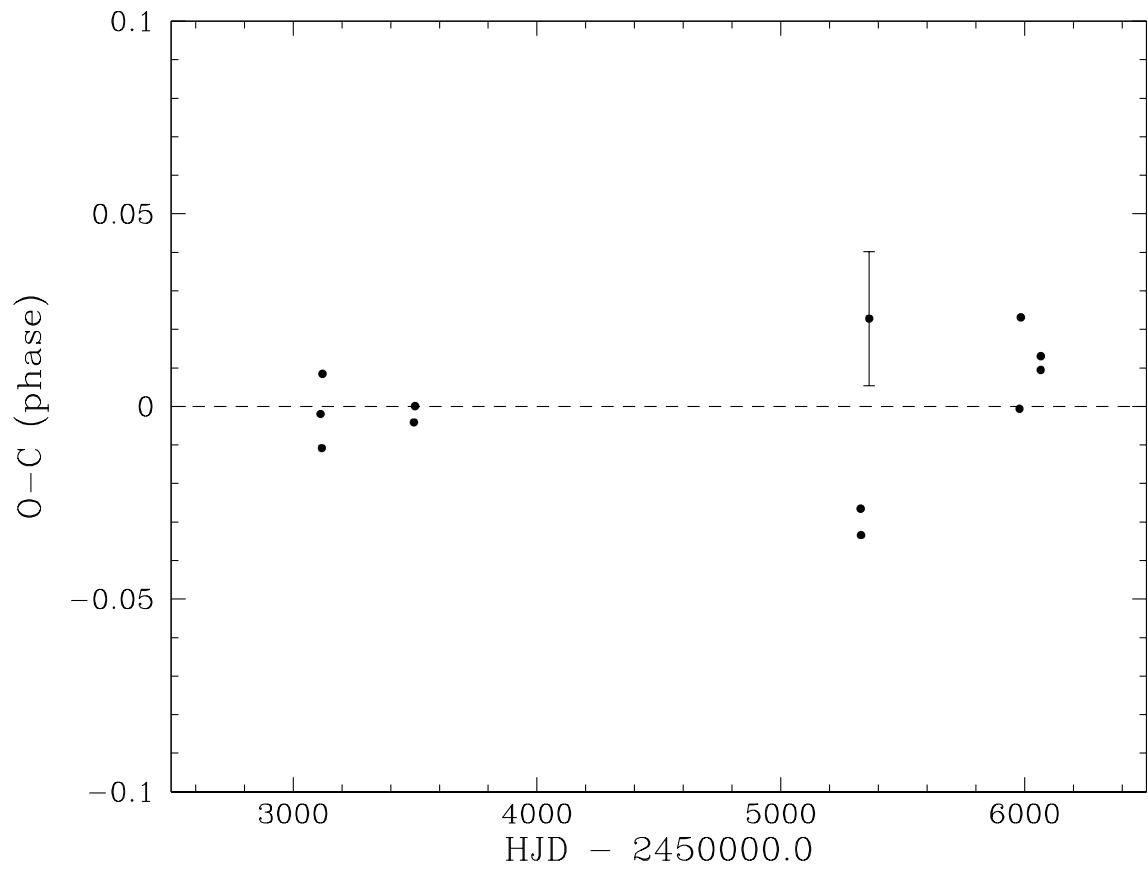


Fig. 3.— Shows that

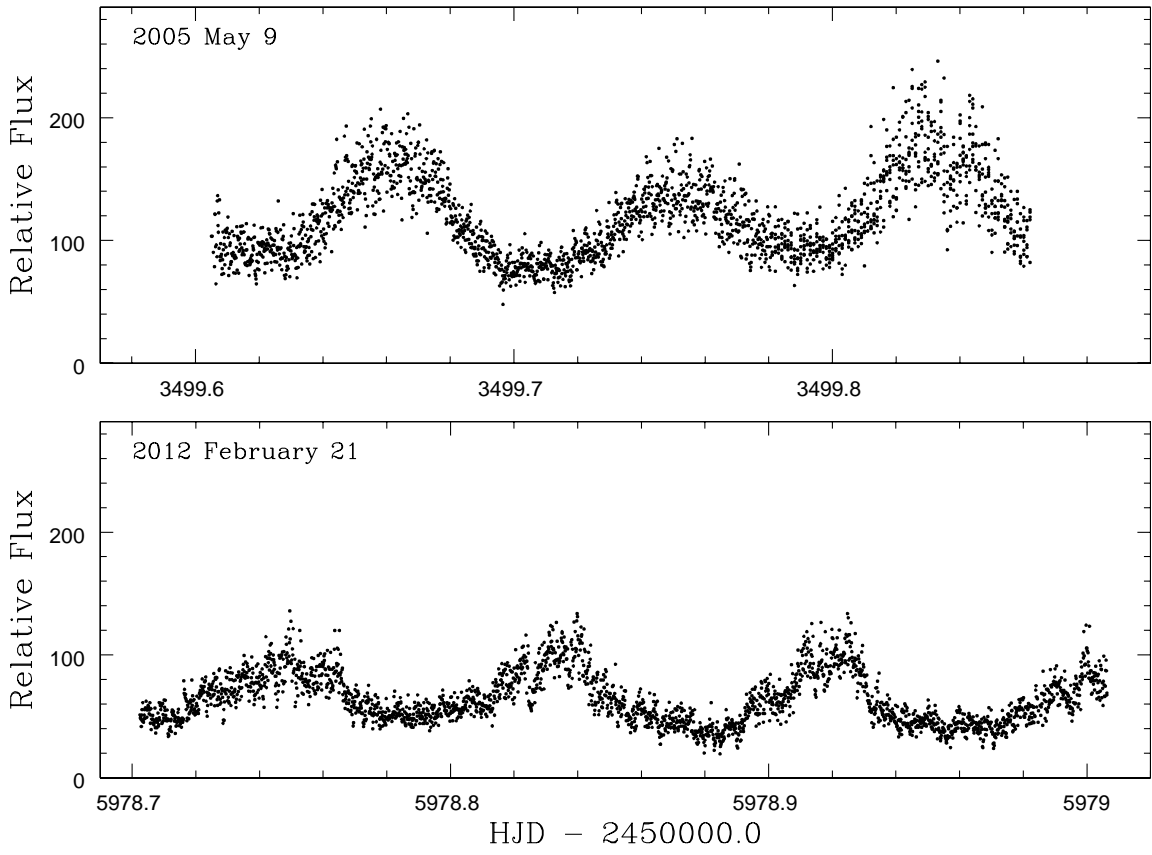


Fig. 4.— Shows that

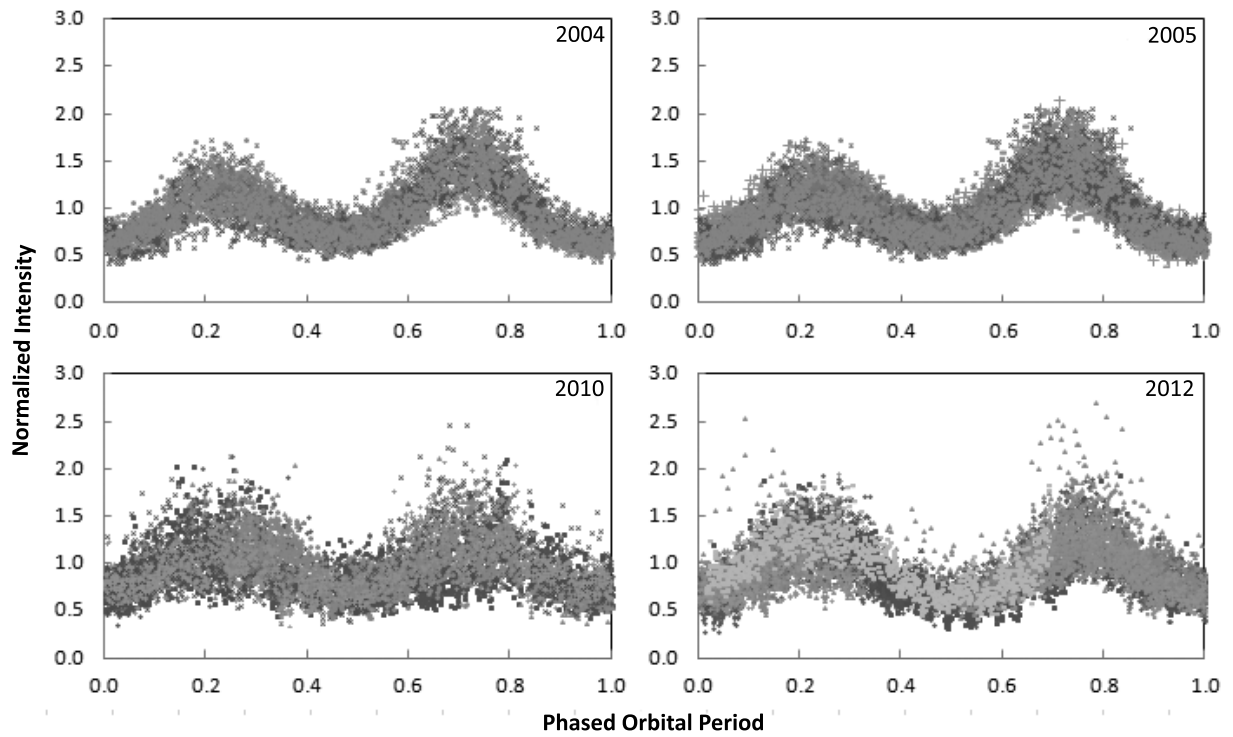


Fig. 5.— Phased yearly data. The phased year data is compiled data from individual phased data. The individual data was then overlapped by the year the data was taken. This was done to verify the result that was given by the O-C diagram of $P = 0.16993379(\frac{\pm 50}{-10})E$.

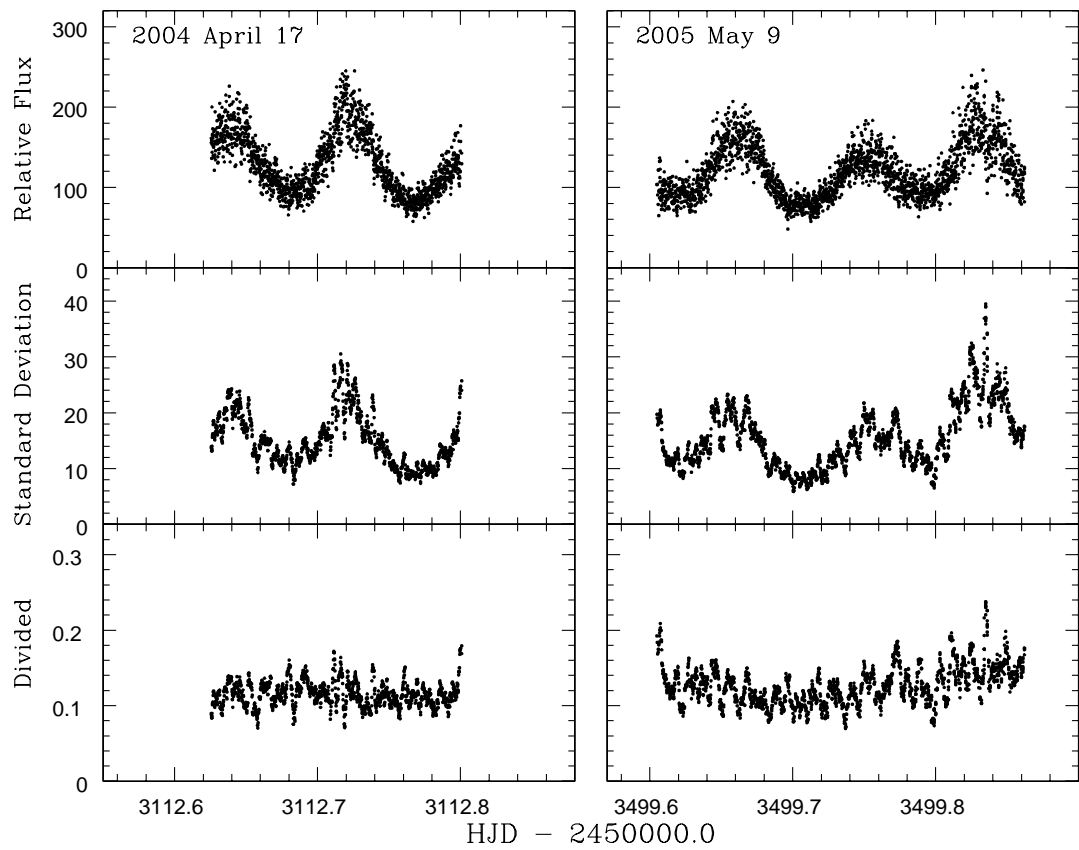


Fig. 6.— 4 Night Light Curves. These four nights were the best 4 nights of data taken in their respective years compared to the other nights. These light curves show how the intensity has decreased from 2004 to 2012. It also shows the sinusoidal variations in the data that was taken.

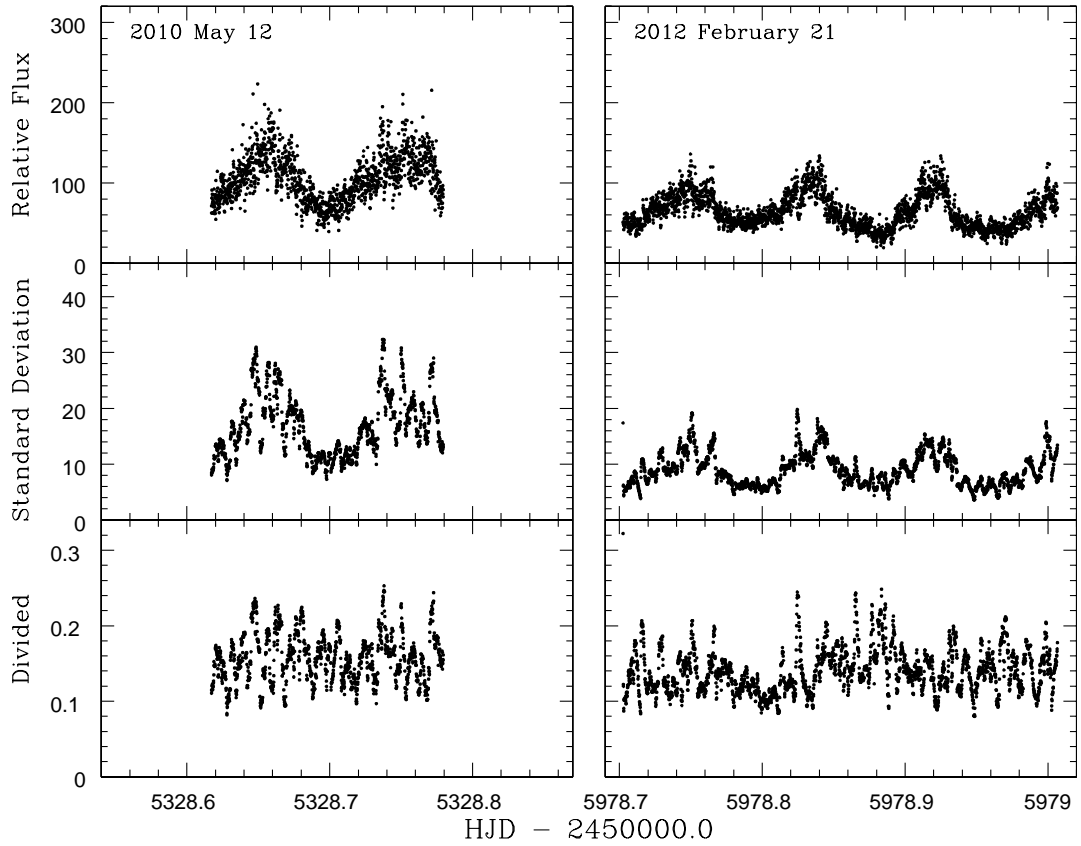


Fig. 7.— Optical variability of J1118+480 is shown two different ways. The dark plots are running standard deviations for 25 photometry points, the same light curves in Figure 5. The light curves are the standard deviation - the dark curve - divided by the average of the 25 10-second photometry points. Notice that the dark curves look very similar to the light curves shown in Figure 5. However, the variability flattens out (light curves) when divided by the mean intensity.

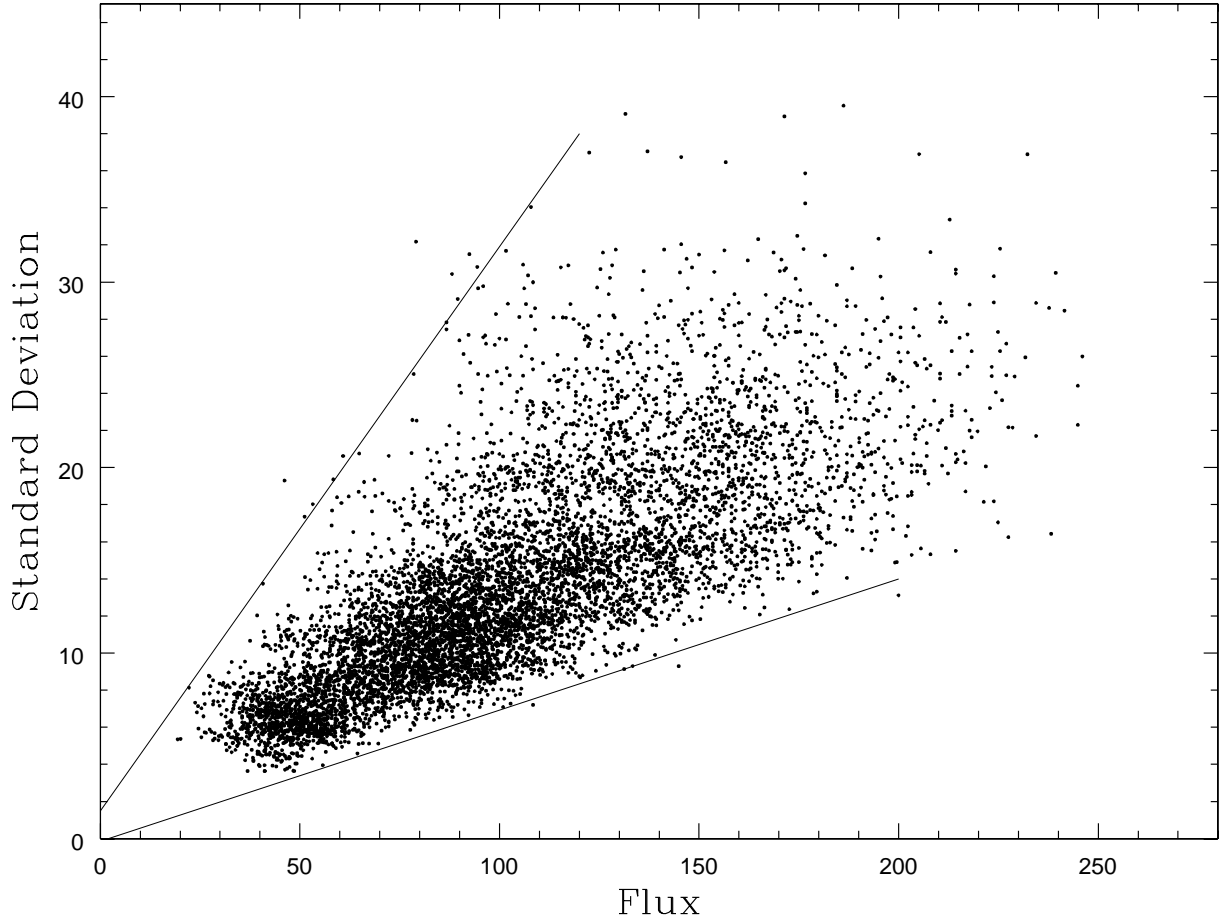


Fig. 8.— The standard deviations from the 4 nights shown in Figure 6 are plotted vs. flux. The standard deviations evolved from the middle of the diagram towards the bottom left corner over time, indicating a gradual decrease in flickering as well as flux. They are as follows (left to right): 2012, 2010, 2005, and 2004.

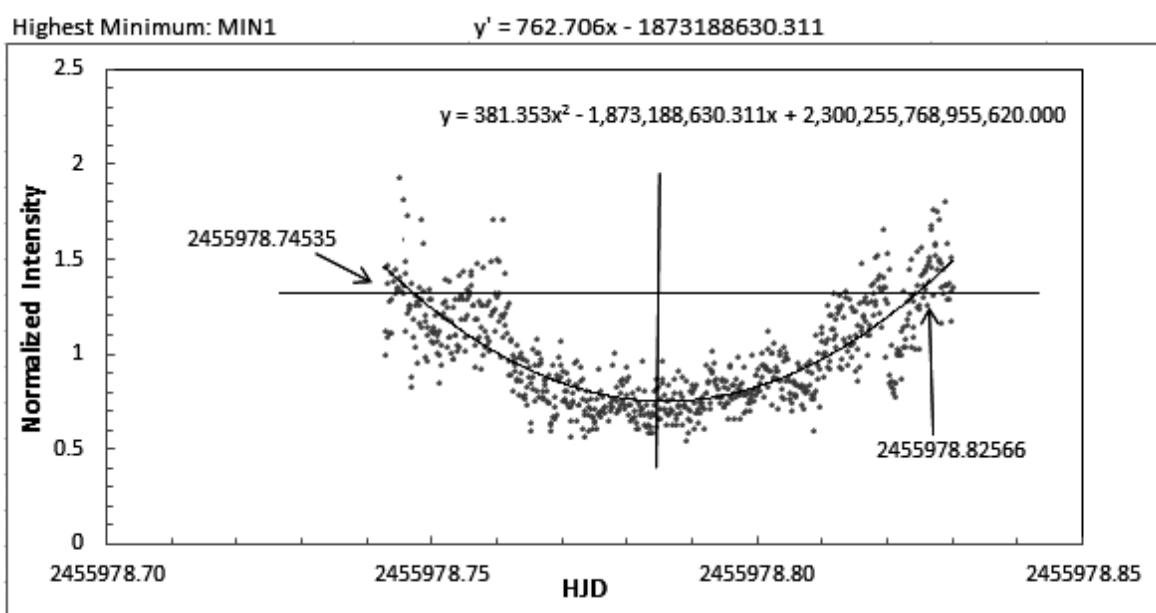


Fig. 9.— Fit example for O-C diagram. To help determine the orbital period the maxima and minimas were taken from all data that showed a well-defined parabola. A parabolic fit was used to determine were the center of the parabola was to insure the correct points were used in the O-C diagram.

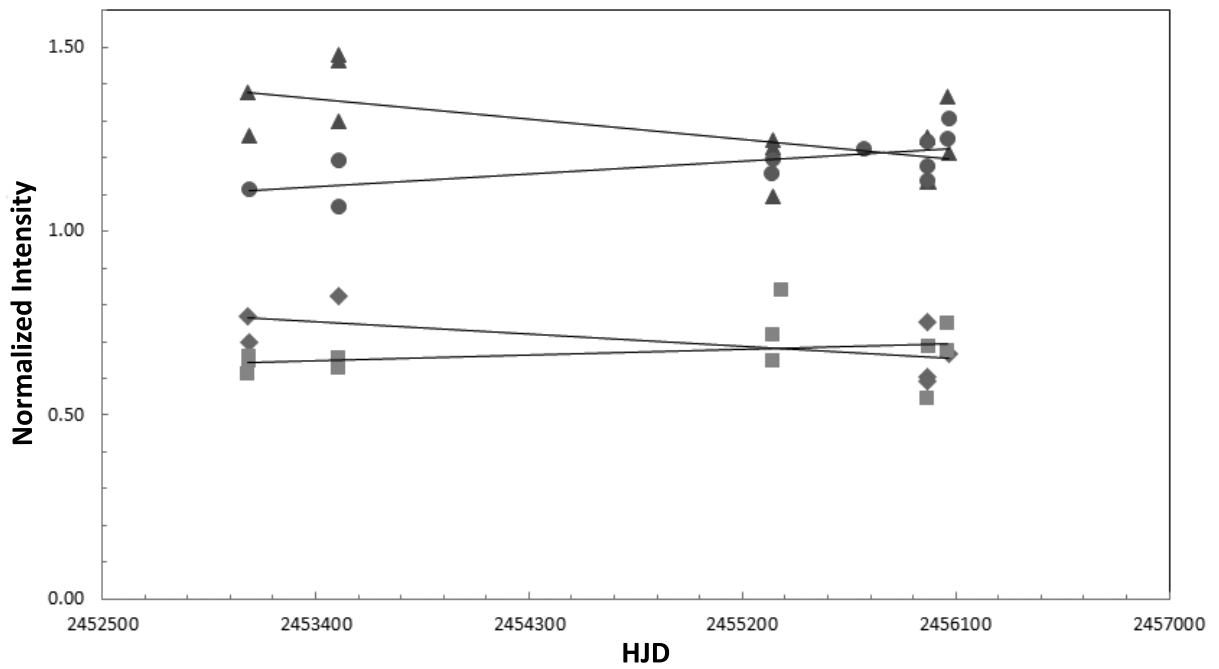


Fig. 10.— Max and Min for all data. Coded as follows: triangle (primary maxima), circle (secondary maxima), diamond (secondary minima), and square (primary maxima). This data gives us an idea on how the binary system is working...and more to add later. XD

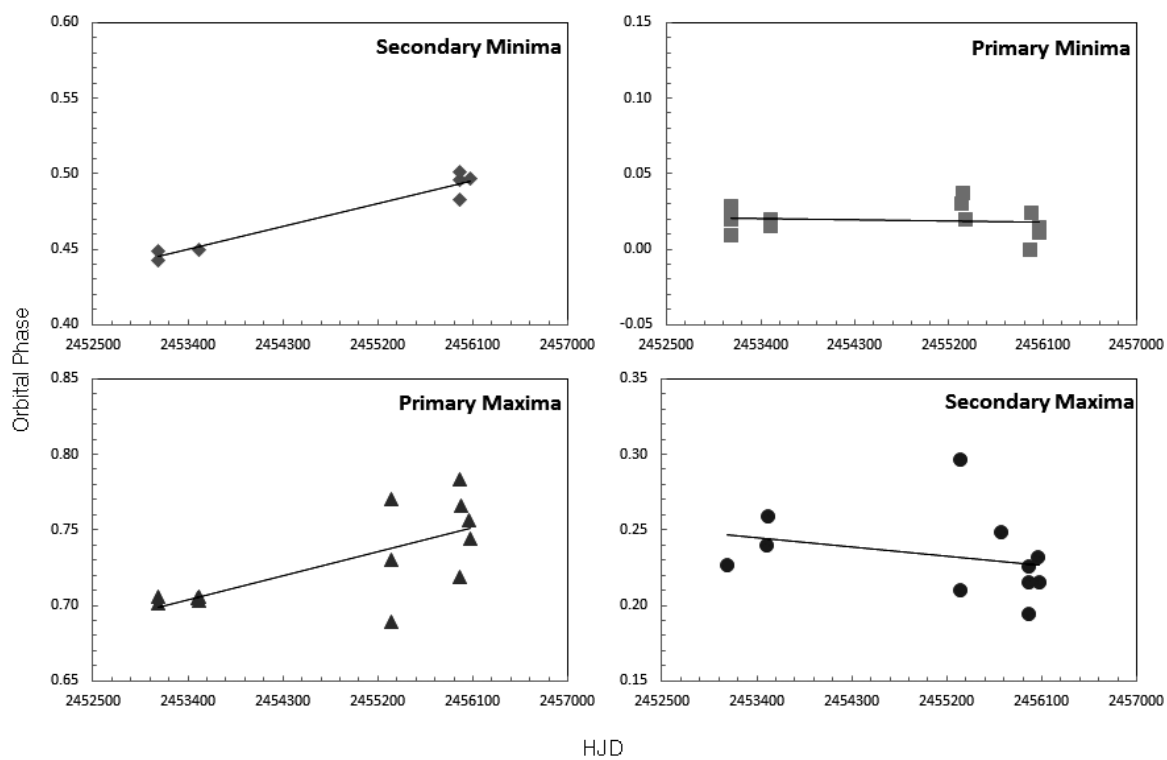


Fig. 11.— Max and Min. This data uses the points from Table 2. It shows the change in the primary and secondary maximas and minimas.

Table 1. Journal of Observations

UT Date	UTC Start	UTC End	Duration (hr)	Exposure Time (sec)
2004 April 17.....	02:55	07:15	~ 4.3	10
2004 April 21.....	04:18	07:47	~ 3.5	10
2004 April 22.....	02:34	07:30	~ 4.1	10
2004 April 23.....	02:27	05:19	~ 2.9	10
2004 April 24.....	02:30	04:41	~ 2.2	10
2004 April 25.....	04:59	09:15	~ 4.3	10
2005 May 05.....	02:46	07:48	~ 5.6	10
2005 May 09.....	02:27	08:43	~ 6.3	10
2010 May 08.....	03:00	06:05	~ 3.0	10
2010 May 11.....	02:52	06:55	~ 4.0	5
2010 May 12.....	02:51	06:48	~ 3.1	10
2010 May 13.....	03:08	06:44	~ 3.6	10
2010 May 14.....	02:50	03:27	~ 0.6	10
2010 May 16.....	03:40	04:12	~ 0.5	10
2010 June 10.....	03:18	06:26	~ 3.1	10
2010 June 11.....	03:34	06:03	~ 2.5	10
2010 June 12.....	03:24	04:11	~ 0.8	10
2010 June 13.....	03:13	03:33	~ 0.3	10
2010 June 15.....	03:24	07:26	~ 4.0	10
2010 June 18.....	03:18	07:00	~ 3.7	10
2011 June 02.....	02:57	04:48	~ 1.9	10
2012 Feb 21.....	04:36	11:58	~ 7.4	10
2012 Feb 22.....	04:56	09:13	~ 4.3	10
2012 Feb 27.....	05:36	09:12	~ 3.6	10
2012 May 16.....	03:57	05:53	~ 2.0	10
2012 May 17.....	03:51	05:46	~ 1.9	10
2012 May 18.....	03:46	05:53	~ 2.1	10
2012 May 19.....	03:56	06:43	~ 3.0	10
2012 May 21.....	04:45	06:05	~ 1.3	10
2012 May 22.....	02:54	05:40	~ 2.8	10

Table 2. Measurements of Max & Mins

Extrema	HJD	Relative Intensity	Phase
Primary Minima	2453112.767	0.61248	0.020
	2453117.694	0.64632	0.029
	2453120.756	0.65843	0.009
	2453495.798	0.62798	0.020
	2453499.707	0.65540	0.015
	2455327.682	0.71613	0.030
	2455328.701	0.64895	0.037
	2455362.697	0.84006	0.019
	2455978.874	0.54351	0.0
	2455984.826	0.68790	0.024
	2456065.712	0.74920	0.011
	2456066.732	0.67307	0.014
	Secondary Maxima	2453120.796	1.11304
2453495.672		1.19110	0.240
2453499.754		1.06539	0.259
2455324.679		1.15539	0.297
2455327.723		1.19671	0.210
2455714.669		1.22395	0.249
2455978.740		1.17545	0.215
2455978.912		1.24224	0.226
2455979.757		1.13795	0.195
2456063.710		1.25289	0.232
2456069.655		1.30748	0.215
Secondary Minima	2453112.677	0.76752	0.449
	2453120.833	0.69745	0.443
	2453499.786	0.82320	0.450
	2455978.786	0.75198	0.482
	2455978.958	0.60563	0.496
	2455979.809	0.59173	0.501
	2456069.703	0.66748	0.497
Primary Maxima	2453112.720	1.37750	0.701
	2453117.649	1.26023	0.706
	2453495.751	1.47893	0.704
	2453499.659	1.29870	0.703
	2453499.830	1.46389	0.706

Table 2—Continued

Extrema	HJD	Relative Intensity	Phase
Primary Maxima	2455327.649	1.09393	0.770
	2455328.654	1.22804	0.689
	2455329.681	1.24745	0.730
	2455978.826	1.25662	0.719
	2455979.857	1.13272	0.783
	2455984.782	1.13377	0.766
	2456066.688	1.36477	0.757
	2456068.725	1.21368	0.744